Probing the Electrostatic Shielding of DNA with Capillary Electrophoresis

Earle Stellwagen and Nancy C. Stellwagen
Department of Biochemistry, University of Iowa, Iowa City, Iowa 52242

ABSTRACT The free solution mobility of a 20-bp double-stranded DNA oligomer has been measured in diethylmalonate (DM) and Tris-acetate buffers, with and without added NaCl or TrisCl. DM buffers have the advantage that the buffering ion is anionic, so the cation composition in the solution can be varied at will. The results indicate that the free solution mobility of DNA decreases linearly with the logarithm of ionic strength when the ionic strength is increased by increasing the buffer concentration. The mobility also decreases linearly with the logarithm of ionic strength when NaCl is added to NaDM buffer or TrisCl is added to TrisDM buffer. Nonlinear effects are observed if the counterion in the added salt differs from the counterion in the buffer. The dependence of the mobility on ionic strength cannot be predicted using the Henry, Debye-Hückel-Onsager, or Pitts equations for electrophoresis. However, the mobilities observed in all buffer and buffer/salt solutions can be predicted within ~20% by the Manning equation for electrophoresis, using no adjustable parameters. The results suggest that the electrostatic shielding of DNA is determined not only by the relative concentrations of the various ions in the solution, but also by their equivalent conductivities.

INTRODUCTION

DNA is a highly charged biopolymer that is found in a variety of electrostatic environments in the cell. To better understand the physical properties of DNA, and how it interacts with proteins and other charged molecules in the cell, it is necessary to understand the electrostatic shielding caused by the small ions in the surrounding media. In most cases of practical interest, the electrolyte concentration in the solution is significantly greater than the DNA concentration. Therefore, the negatively charged DNA molecules will be surrounded by a diffuse ion atmosphere that modulates its interaction with other charged molecules in the solution and with externally applied electric fields. The thickness of the ion atmosphere is usually characterized by the Debye-Hückel parameter κ^{-1}, which varies inversely with the square root of ionic strength (Bockris and Reddy, 1998).

A convenient method of measuring the electrostatic shielding of DNA, and the changes in electrostatic shielding caused by changes in electrolyte concentration, is to determine the free solution mobility using capillary electrophoresis (Stellwagen and Stellwagen, 2002). The free solution mobility of DNA (and other analytes) is determined by the ratio of the effective charge of the ion to its friction coefficient, as shown in Eq. 1:

$$\mu = q/f, \tag{1}$$

where μ is the mobility, q is the effective charge, and f is the friction coefficient (review: Viovy, 2000). However, the observed mobility is reduced by two effects usually called the ''relaxation effect'' and the ''electrophoretic effect'' (Onsager and Fuoss, 1932; Manning, 1981; Bockris, 1998). The relaxation effect is related to the induced dipole caused by the electric field-induced separation of the center of charge of the counterions from the center of charge of the macromolecule. The induced dipole, in effect, creates an internal electric field that opposes the external field, decreasing the effective amplitude of the external field (Jumppanen and Riekkola, 1995). The electrophoretic effect is caused by the migration of the solvated counterions and the polyion in opposite directions. The migration of the counterions creates a source of viscous drag in addition to that caused by the migration of the polyions.

In our initial studies of the electrostatic shielding of DNA, the free solution mobility of linearized pUC19 (2686 bp) and a 20-bp double-stranded oligomer called dsA5 were measured in Tris-acetate-EDTA (TAE) buffers of various concentrations (Stellwagen and Stellwagen, 2002). The electrophoretic mobilities of the two DNAs decreased monotonically with the conductivity of the solution when the TAE buffer concentration was increased from 10 to 400 mM. However, when the conductivity was increased by adding NaCl to a constant concentration of TAE buffer, very unusual effects were observed. The mobilities of the two DNAs increased slightly when 2 mM NaCl was added to 18 mM TAE buffer, remained approximately constant when the NaCl concentration was increased from 2 to 50 mM, and then began to decrease at NaCl concentrations of 75 mM and higher. The constant mobilities observed in the mixed NaCl-TAE buffer solutions occurred over the same range of ionic strengths where the mobilities progressively decreased when the ionic strength (or conductivity) was increased by increasing the TAE buffer concentration. Inasmuch as very similar results were observed for linear pUC19 and dsA5 in all TAE and TAE/NaCl solutions, these unusual electrostatic shielding effects are independent of DNA molecular weight.

To better understand this unusual dependence of DNA mobility on the ionic strength and composition of the

Submitted September 4, 2002, and accepted for publication November 6, 2002.

Address reprint requests to Nancy C. Stellwagen, Dept. of Biochemistry, Univ. of Iowa, 51 Newton Rd., Iowa City, IA 52242. Tel.: 319-335-7896; Fax: 319-335-9570; E-mail: nancy-stellwagen@uiowa.edu.

0006-3495/03/03/1855/12 $2.00

electrolyte, the mobility of dsA5 has now been measured in diethylmalonate (DM) buffer solutions, with and without added NaCl or TrisCl. Since the buffering ion in this system is anionic, solutions containing a single counterion can be prepared by titrating diethylmalonic acid with the hydroxide of the counterion of choice.

The results indicate that the free solution mobility of DNA decreases linearly with the logarithm of ionic strength when the ionic strength is increased by increasing the DM buffer concentration. The mobility also decreases linearly with the logarithm of ionic strength when Na^+ ions are added to sodium diethylmalonate (NaDM) buffer or $Tris^+$ ions are added to Tris diethylmalonate (TrisDM) buffer. Anomalous mobility effects are observed only when the counterion in the added salt differs from the counterion in the buffer. The mobility of DNA decreases more slowly than expected when the ionic strength of the solution is increased by adding a counterion with a higher equivalent conductivity than the counterion in the buffer; conversely, the mobility decreases more rapidly than expected when the ionic strength is increased by adding a counterion with a lower equivalent conductivity than that of the buffer counterion.

Attempts were also made to predict the ionic strength dependence of the mobility in the various buffer and buffer/salt solutions, using several equations in the literature. The Henry and Debye-Hückel-Overbeek equations (Li et al., 1999) predict that the mobility should decrease linearly with the square root of ionic strength. Such plots are highly curvilinear, indicating that these theories are not good predictors of the mobilities observed in the relatively high ionic strength solutions used for electrophoresis. However, plots of the inverse mobility as a function of ionic strength are linear over the entire range of ionic strengths examined here, 5–200 mM. Extrapolating the various mobility plots to zero ionic strength, the intrinsic mobility of the 20-bp oligomer dsA5 is found to be $(4.6 \pm 0.2) \times 10^{-4}\ cm^2\ V^{-1}\ s^{-1}$, independent of the buffer in which the measurements are made.

The mobilities observed for dsA5 in the various buffer solutions were also compared with the predictions of the Pitts theory (Pitts, 1953; Pitts, et al., 1970; Li et al., 1999). This equation includes an additional adjustable parameter that can be used to linearize the mobilities observed at finite buffer concentrations. However, the same parameters cannot be used to predict the mobilities observed in buffer/salt solutions with mixed cations.

The Manning electrophoresis theory is very different from the other theories, predicting that the mobility should decrease with the logarithm of increasing ionic strength, not the square root. The mobilities calculated from the Manning equation, which uses no adjustable parameters, agree with the experimentally observed mobilities within 20% over the whole range of ionic strengths investigated. Importantly, the anomalous mobilities observed in buffer/salt solutions with mixed counterions can also be predicted from the Manning electrophoresis theory, if the relative concentrations and equivalent conductivities of the various ions in the solution are taken into account. The results indicate that the electrostatic shielding of DNA is determined not only by the relative concentrations of the various ions in the solution, but also by their equivalent conductivities (or transference numbers).

MATERIALS AND METHODS

DNA samples

The ds20-bp oligomer used in these studies was 5′-CGCAAAAACGCG-CAAAAACG-3′. The oligomer and its complement were synthesized by standard methods (Integrated DNA Technologies, Coralville, IA), purified by polyacrylamide gel electrophoresis, electroeluted from the gel, lyophilized, redissolved at a concentration of 100 μM in 10 mM TrisCl buffer, pH = 7.6, and stored at −20°C until needed. The two strands were annealed by heating equimolar quantities of each oligonucleotide in a water bath at 80°C for 5 min and slowly cooling the solution to room temperature. Double-strand formation was verified by polyacrylamide gel electrophoresis in gels containing 9.3% w/v total acrylamide (*%T*, *T* = acrylamide + crosslinker) and 3% w/w *N*,*N*′-methylenebisacrylamide (Bis) crosslinker (*%C*, *C* = *[Bis]/[T]*), comparing the mobility of the annealed oligomer with that of the fragments in a 10-bp ladder (Invitrogen, Carlsbad, CA). The methods used for casting and running polyacrylamide gels have been described previously (Stellwagen, 1998). Concentrated stock solutions of dsA5 were diluted to 20–100 ng/μL with T0.1E buffer (10 mM TrisCl buffer, 0.1 mM EDTA, pH 8.1), just before the capillary electrophoresis measurements were begun. The results were independent of DNA concentration within this range.

Adenosine 3′,5′-cyclicmonophosphate (cAMP) and adenosine 5′-carboxylic acid (ACA) were purchased from Sigma (St. Louis, MO) and used without further purification.

Buffers and buffer/salt mixtures

Two neutral pH buffers, Tris and DM, were used as background electrolytes in the present work. Diethylmalonic acid, which has not previously been used to study the electrophoresis of DNA, has the chemical formula $(CH_3CH_2)_2C(COOH)_2$. Stock solutions of the various buffers were prepared according to the following recipes: Tris acetate (TA), 400 mM Tris base brought to pH 8.0 with glacial acetic acid; TAE, 400 mM Tris base brought to pH 8.0 with glacial acetic acid, plus 10 mM EDTA; TrisDM, 100 mM diethylmalonic acid brought to pH 7.3 with Tris base; NaDM, 500 mM diethylmalonic acid brought to pH 7.30 with NaOH. More dilute buffers were prepared by dilution of the concentrated stock solutions. To prepare mixed buffer/salt solutions with a constant buffer concentration, suitable volumes of 100 mM NaCl or 200 mM TrisCl in 5 mM NaDM were added to suitable volumes of 5 mM NaDM; 100 mM NaCl in 10 mM TrisDM was added to 10 mM Tris DM; 100 mM TrisCl in 5 mM TrisDM was added to 5 mM Tris DM; and 100 mM NaCl dissolved in 18 mM TAE buffer was added to 18 mM TAE buffer.

The ionic strengths of solutions containing Tris buffers of various concentrations were calculated from the measured pH and the known pK_a of the Tris ion, 8.3 at 20°C (Good et al., 1966). Because the buffering ion is singly charged, TA and TAE buffers at pH = 8.3 have an ionic strength equal to one-half the total Tris concentration. The DM ion contains two carboxyl groups, one completely ionized at neutral pH and another with a pK_a of 7.3 at 25°C (Sober, 1968). Therefore, the DM ion carries one negative charge plus the fractional charge calculated from the pH of the solution and the pK_a of the buffering ion. At pH = 7.3, the ionic strength of a DM solution is equal to twice the nominal DM concentration. The ionic strengths of buffers and salts in mixed buffer/salt solutions were assumed to be additive.

Capillary electrophoresis

Capillary zone electrophoresis was carried out with a Beckman Coulter P/ACE System MDQ Capillary Electrophoresis System (Fullerton, CA), operated in the anodic migration mode (positive electrode on the outlet side) with UV detection at 254 nm, close to the absorption maximum of DNA. Migration times and peak profiles were analyzed using the MDQ-32 Karat software with the Caesar algorithm. Two capillaries were used during the course of the present work. The first had a length of 39.3 cm (29.1 cm to the detector); the second was 39.1 cm long (29.1 cm to the detector). Both capillaries were neutral eCAP capillaries (Beckman) coated with polyacrylamide and had external diameters of 350 μm and internal diameters of 100 μm. No sieving liquid polymers were used in these experiments; the capillary was filled with buffer alone. The capillary was conditioned at the beginning of each day by rinsing with running buffer for 2 min at high pressure (25 psi, 0.17 MPa, >18 column volumes). Between runs, the capillary was rinsed with running buffer at 25 psi for 1 min. The capillary was flushed with deionized water at 25 psi for 5 min at the end of each day and filled with deionized water overnight.

All DNA samples were hydrodynamically injected into the capillary using a 3-s injection at low pressure (0.5 psi, 0.0035 MPa); the sample plug comprised 0.9% of the column volume. The applied electric field was usually 150–200 V/cm if the buffer concentration was 40 mM or less; lower voltages were used for more concentrated buffer and buffer/salt solutions to keep the current below 35 μA, both to preserve the capillary coating and to prevent Joule heating. The observed mobilities were constant within $\pm$ 2% when the electric field strength was varied from 50–200 V/cm. The capillary was thermostated at 20.0 $\pm$ 0.1°C for all experiments.

Calculations

The electrophoretic mobilities of dsA5 in the various buffer and buffer/salt solutions were calculated from Eq. 2:

$$\mu = d/Et, \tag{2}$$

where μ is the observed mobility, d is the distance to the detector (in cm), E is the electric field strength (in V/cm), and t is the time required for the sample to travel to the detector (in seconds). In most cases, the electroosmotic flow of the solvent (EOF) was very low and could be neglected with respect to the mobility of the DNA. However, deterioration of the capillary coating toward the end of the studies led to a small but measurable EOF in some experiments. The observed mobilities, μ_{obs}, were then corrected by Eq. 3:

$$\mu_{obs} = \mu_{DNA} - \mu_{EOF}, \tag{3}$$

where μ_{DNA} is the true electrophoretic mobility of the DNA and μ_{EOF} is the mobility due to the EOF (Grossman, 1992). The EOF mobility was estimated by comparing the known mobility of dsA5 in 40 mM TAE buffer (Stellwagen and Stellwagen, 2002) with the mobility observed in the same buffer during the course of the measurements.

The viscosities of the more concentrated buffer and buffer/salt solutions used in this study differed measurably from the viscosity of pure water. Therefore, the measured mobilities were corrected for the viscosity of the solvent using Eq. 4:

$$\mu_{corr} = \mu_{meas} \times \eta_{water}/\eta_{soln}, \tag{4}$$

where μ_{corr} is the corrected mobility, μ_{meas} is the measured mobility in the buffer/salt solution, η_{soln} is the relative viscosity of the buffer/salt solution compared to the viscosity of pure water, and η_{water} is the viscosity of water at 20°C, the temperature of the measurements. The relative viscosities of Tris-acetate buffers of various concentrations were estimated from the average relative viscosities of Tris and Na acetate solutions (which are nearly equal), taken from standard tables (Weast, 1984). The relative viscosities of DM solutions have not been measured, to the authors' knowledge. It was assumed for the present purposes that the relative viscosities of the DM solutions could be approximated by averaging the relative viscosities of Na_2HPO_4 and NaH_2PO_4 solutions of the same concentration (Weast, 1984), because phosphate buffers also contain a mixture of mono- and divalent buffering ions. Solutions containing low concentrations of buffer and excess NaCl were assumed to have the relative viscosity of NaCl solutions of the appropriate concentration (Weast, 1984); solutions with added TrisCl were assumed to have the relative viscosity of Tris. The viscosity corrections amounted to 5% or less of the observed mobilities, even at the highest buffer and salt concentrations used in the present study.

The limiting equivalent conductivities of the various ions used in this study are given in Table 1. Because the equivalent conductivities were measured at 25°C, and the present measurements were carried out at 20°C, the literature values were corrected to a temperature of 20°C by multiplying by the ratio of the viscosity of water at the two temperatures, according to Eq. 5:

$$\lambda^{o}_{20} = \lambda^{o}_{25}(\eta_{25}/\eta_{20}) = 0.8886\,\lambda^{o}_{25}. \tag{5}$$

The limiting equivalent conductivity of DM has not been measured. However, ethylmalonate and ½ dimethylmalonate have virtually identical equivalent conductivities (Weast, 1984), so the latter was taken as the equivalent conductivity of ½ DM.

Comparison with electrophoresis equations in the literature

To better understand how electrophoretic mobilities relate to electrostatic shielding effects, the mobilities observed in the various buffer and buffer/salt solutions have been compared with the mobilities calculated from several equations in the literature.

Henry equation

The electrophoretic mobility of a spherical polyion in very dilute salt solutions is often described by the Henry equation:

$$\mu = \frac{Qf(\kappa a)}{4\pi\eta a(1+\kappa a)} \sim c_1 I^{-1/2}, \tag{6}$$

where μ is the mobility, Q is the effective charge of the polyion, κ is the inverse of the Debye screening length, a is the polyion radius, and η is the viscosity of the solution (Henry, 1931; Weime, 1975; Russel et al., 1989). Because $f(\kappa a)$ is a small number ranging between 2/3 and 1, and κ is proportional to $I^{1/2}$, the electrophoretic mobility of a polyion is predicted to decrease as $I^{1/2}$ for sufficiently large values of (κa). Although such plots are usually curved (Friedl et al., 1995; Li et al., 1999), they are commonly used to extrapolate the observed mobilities to infinite dilution and obtain the intrinsic mobility of an analyte. The constant c_1 characterizing the initial decrease of the mobility as a function of $I^{1/2}$ is known as the Onsager limiting slope.

TABLE 1 Limiting ionic conductivities

Ion	λ^{o}_{25}, cm^2 S eq^{-1}	λ^{o}_{20}, cm^2 S eq^{-1}
Na	50.1*	44.5
Tris	29.72†	26.4
Acetate	40.9*	36.3
Cl	73.51*	65.3
½ DM‡	49.4*	43.9

*Infinite dilution at 25°C (Weast, 1984).
†Taken from (Klein and Bates, 1980; Ng and Barry, 1995).
‡Approximated by the value for ½ dimethyl malonate (Weast, 1984).

Debye-Hückel-Onsager (DHO) equation

Onsager used the ion atmosphere model introduced by Debye and Hückel to derive an expression for the equivalent conductance of an analyte, which can be related to electrophoretic mobility through Eq. 7:

$$\mu_i^o = \lambda_i^o/F, \tag{7}$$

where μ_i^o is the mobility of ion i at infinite dilution, λ_i^o is the limiting equivalent conductivity of the ion, and F is the Faraday constant (Bockris and Reddy, 1998). Recasting the DHO equation in terms of mobilities and evaluating the terms for aqueous solutions at 20°C gives:

$$\mu = \mu^o - [(3.125 \times 10^4) + 0.229\mu^o]I^{1/2}, \tag{8}$$

where μ is the mobility of the polyion at finite ionic strength (in units of 10^{-4} cm^2 V^{-1} s^{-1}) and μ^o is the mobility at zero ionic strength (Li et al., 1999; Porras et al., 2002).

Pitts equation

Pitts derived an expression for the equivalent conductance of an ion of finite size based on the Debye-Hückel limiting law (Pitts, 1953; Pitts et al., 1970). Li et al. (1999) have simplified this equation and applied it to electrophoresis, giving rise to the following expression for aqueous solutions at 20°C:

$$\mu_i = \mu_i^o - \left(3.125 \times 10^{-4} z_i + \frac{0.391|z_i|2q\mu_i^o}{(1 + q^{1/2})}\right) \times \frac{I^{1/2}}{(1 + BaI^{1/2})}, \tag{9}$$

where μ_i is the mobility of the analyte (in cm^2 V^{-1} s^{-1}), μ_i^o is the mobility of the analyte at infinite dilution, z_i is the charge on the buffer anion, q is a parameter related to electrolyte type, B is a group of constants equal to 0.3291 Å^{-1} M$^{-1/2}$, and a is an ion size parameter describing the distance of closest approach between an analyte and its counterion. The ion size parameter is usually treated as an adjustable parameter and fitted to the mobility data. The Pitts equation can be written in simplified form (Li et al., 1999) as:

$$\mu_i = \mu_i^o - c_1[I^{1/2}/(1+c_2\, I^{1/2})], \tag{10}$$

where c_1 is the Onsager limiting slope and c_2 is an adjustable constant, determined from plots of the mobility as a function of $I^{1/2}/(1 + c_2\, I^{1/2})$.

Manning equation

Manning (1981) derived an equation for the electrophoretic mobility of DNA based on the polyelectrolyte nature of the analyte, taking into account the electrophoretic and relaxation effects described above. This equation is:

$$\mu = (300z_1)^{-1}[\varepsilon\varepsilon_o kT/(3\pi\eta p)]|\ln(\kappa b)|(\alpha/\beta), \tag{11}$$

where z_1 is the valence of the counterion, ε is the dielectric constant of the solvent, ε_o is the permittivity of vacuum, k is Boltzmann's constant, T is the absolute temperature, η is the viscosity of the solution, p is the protonic charge, κ is the inverse of the Debye screening length, and b is the axial charge spacing of the polyion. The parameters α and β are defined as:

$$\alpha = 1 - 1/3\ \nu_1(\nu_1+\nu_2)^{-1}|z_1z_2|^{-1}(z_1^2 - z_2^2) \tag{12}$$

$$\beta = 1+108\ \nu_1(\nu_1+\nu_2)^{-1}|z_1z_2|^{-1}(z_1)^{-1} [\varepsilon\varepsilon_o kT/(3\pi\eta p)]|\ln(\kappa b)|(z_1^2/\lambda_1 + z_2^2/\lambda_2), \tag{13}$$

where ν_1 and ν_2 are the number of ions of species i in the electrolyte, z_1 and z_2 are the valences of the counterions ions and coions, respectively, and λ_1 and λ_2 are the limiting ionic conductivities of the counter- and coions. In solutions containing multiple cations and/or anions, it is necessary to multiply the individual values of z_i^2/λ_i in the last term in Eq. 13 by the mole fraction of each counterion or coion in the solution. Note that the Manning equation, Eqs. 11–13, predicts that the mobility should decrease as the logarithm of ionic strength (through *ln* κ), not the square root of ionic strength as predicted by the other theories. In addition, the Manning equation contains no adjustable parameters, only numerical constants and known quantities such as the axial charge density of DNA and the limiting equivalent conductivities of the ions, which are available from standard tables. Hence, the mobilities calculated from Eqs. 11–13 can be compared directly with experiment, providing a stringent test of the validity of the Manning equation.

Other treatments of electrophoretic mobility

Various other treatments have been devised to describe the dependence of electrophoretic mobility on the composition of the solvent. Some of these treatments are purely empirical (e.g., Reijenga and Kenndler, 1994). Other equations are based on the Debye-Hückel approximation and include the ζ potential, an ill-defined quantity describing the electric potential at the shear surface of an analyte (Overbeek and Wiersema, 1967; Schellman and Stigter, 1977; Russel et al., 1989; Viovy, 2000). The ζ potential varies with ionic strength and is often treated as an adjustable parameter (Schellman and Stigter, 1977). More recently, numerical boundary element methods have been used to solve the coupled Navier-Stokes, Poisson and ion transport equations, using the translational diffusion coefficients of the analytes to calculate their effective molecular radii (Allison and Mazur, 1998; Mazur et al., 2001). The calculated mobilities have been found to agree with experiment within 6–15%, depending on the buffer used as the background electrolyte. However, extensive computer time is required for the calculations and the method assumes that the Nernst-Einstein relation is valid for free solution electrophoresis, an assumption that is currently a matter of debate (Nkodo et al., 2001).

RESULTS AND DISCUSSION

Electropherograms of dsA5 in Tris and DM buffers, with and without added salt

The peaks observed for dsA5 in Tris and DM buffers of various concentrations were sharp, relatively symmetrical, and approximately Gaussian in shape, as shown in Figs. 1 *a*, 2 *a*, 3 *a*, and 3 *c*. The sharpness and symmetry of the peaks indicate that the oligomer was not interacting with the

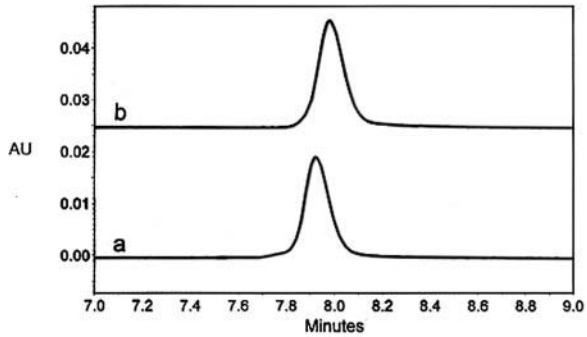

FIGURE 1 Electropherograms observed for dsA5 in 20 mM TAE buffer, pH 8.3, (trace *a*); and in a solution containing 18 mM TAE buffer plus 10 mM NaCl (trace *b*). In both cases, $E = 206$ V/cm.

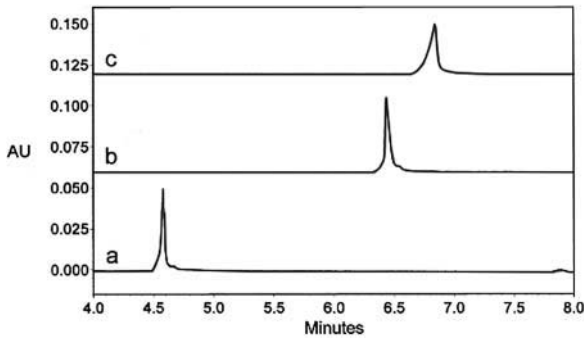

FIGURE 2 Electropherograms observed for dsA5 in 5 mM NaDM buffer, pH 7.3 (trace *a*); 5 mM NaDM plus 10 mM NaCl (trace *b*); and 5 mM NaDM plus 10 mM TrisCl (trace *c*). $E = 206$ V/cm.

components in the Tris and DM buffers (Stellwagen and Stellwagen, 2002). The peaks remained sharp and symmetrical when NaCl was added to Tris and DM buffers (Figs. 1 *b*, 2 *b*, and 3 *c*). However, the peaks became somewhat broader and more skewed in shape when TrisCl was added to NaDM or TrisDM, as shown in Figs. 2 *c* and 3 *b*, respectively.

Forward-fronting of the peaks observed in capillary electrophoresis is usually attributed to electromigration dispersion in front of the sample zone and isotachoelectrophoretic stacking of the sample at the rear of the sample zone, and occurs when the mobility of the analyte is faster than the mobility of the coion in the buffer (Beckers and Bŏcek, 2000). With more than one buffer coion, the shape of the analyte peak is determined by the coion with the mobility closest to that to the analyte (Gebauer and Bŏcek, 1997; Beckers et al., 2001). However, as shown in Figs. 2 and 3, these simple rules do not apply to the Na/Tris/DM/Cl buffer system, because the identity of the counterion also affects peak shape. Sharp symmetric peaks are observed when the mixed buffer system contains only Na^+ as the counterion; forward-fronting and broadened peaks are observed when the buffer contains both Na^+ and $Tris^+$ ions. These complicated buffer effects on peak shape will be treated in more detail in a forthcoming publication (manuscript in preparation).

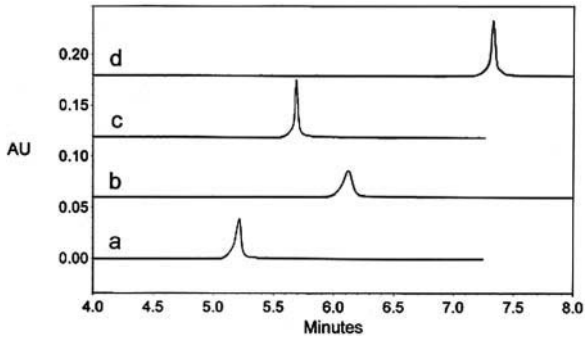

FIGURE 3 Electropherograms observed for dsA5 in 5 mM TrisDM buffer, pH 7.3 (trace *a*); 5 mM TrisDM plus 10 mM TrisCl (trace *b*); 10 mM TrisDM (trace *c*); and 10 mM TrisDM plus 10 mM NaCl (trace *d*). $E = 206$ V/cm.

Intrinsic mobility at zero buffer concentration

The mobilities observed for dsA5 in Tris-acetate, TrisDM, and NaDM buffers of different concentrations are plotted as a function of the square root of ionic strength in Fig. 4 *A*. Although the Henry and DHO equations, Eqs. 6 and 8, predict that the mobility should decrease linearly with $I^{1/2}$, the curves in Fig. 4 *A* are linear only at very low ionic strengths, because of the breakdown of the Debye-Hückel approximation at high ionic strengths. Small electrolytes also exhibit curved plots of mobility versus $I^{1/2}$, for the same reason (Friedl et al., 1995; Li et al., 1999).

In contrast to the curved mobility plots illustrated in Fig. 4 *A*, linear plots are obtained if the inverse mobility is plotted as a function of ionic strength, as shown in Fig. 4 *B*. The theoretical significance of the linearity of these plots is not clear at the present time. However, the inverse mobility is also a linear function of DNA molecular weight in agarose (Southern, 1979; Van Winkle et al., 2002) and polyacrylamide (Southern, 1979) gels. It is possible that these two observations are related.

The intrinsic mobility of dsA5 at zero ionic strength can be estimated by linear extrapolation of the mobilities observed at low buffer concentrations (Fig. 4 *A*), assuming that the limiting slopes of the curves have been reached. The intrinsic mobilities obtained in this manner are given in Table 2,

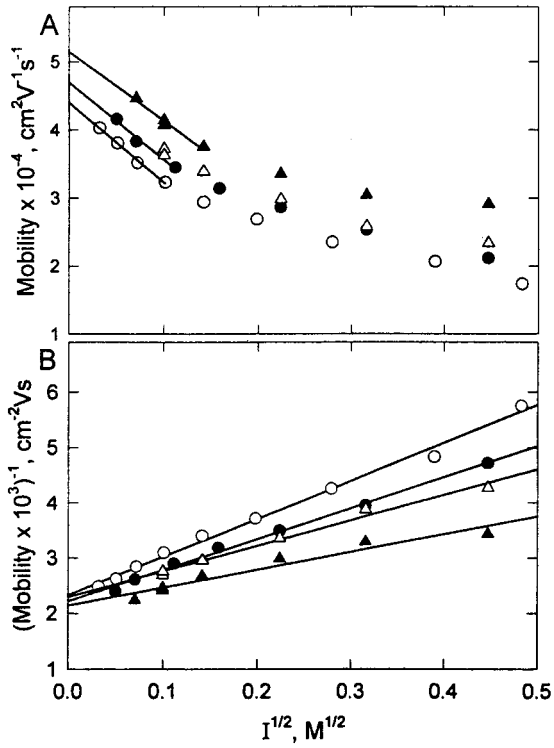

FIGURE 4 Dependence of the electrophoretic mobility of dsA5 on the square root of ionic strength. (*A*) μ versus $I^{1/2}$. (*B*) $1/\mu$ versus $I^{1/2}$. (○), TAE buffer, pH 7.6; (●), TA buffer, pH 8.3; (△), TrisDM buffer, pH 7.3; (▲), NaDM buffer, pH 7.3.

TABLE 2 Intrinsic mobilities and onsager limiting slopes for dsA5

		Fig. 4, Panel A		Panel B	Average*
Buffer	pH	$\mu^o \times 10^4$, $cm^2\ V^{-1}\ s^{-1}$	Onsager slope	$\mu^o \times 10^4$, $cm^2\ V^{-1}\ s^{-1}$	$\langle\mu^o\rangle \times 10^4$, $cm^2\ V^{-1}\ s^{-1}$
TAE	7.6	4.40	11.8	4.29	4.34 ± 0.06
TA	8.3	4.70	11.4	4.51	4.60 ± 0.10
TrisDM	7.3	4.70	11.4	4.36	4.52 ± 0.18
NaDM	7.3	5.15	10.2	4.67	4.91 ± 0.24

*Average values of μ and $1/\mu$ extrapolated to $I^{1/2} = 0$.

column 3; the corresponding Onsager limiting slopes are compiled in column 4. It can be seen that the Onsager slopes are very similar in all buffers except NaDM, where the data do not extend to low enough ionic strengths for accurate extrapolation.

To improve the accuracy of the extrapolation of the mobilities to zero ionic strength, the inverse mobilities in Fig. 4 *B* were also extrapolated to zero ionic strength, with the results shown in Table 2, column 5. The intrinsic mobilities obtained from the two extrapolations were then averaged, as shown in Table 2, column 6. It can be seen that the values of $\langle\mu^o\rangle$ are somewhat dependent on the composition of the buffer. If these small differences are ignored and the intrinsic mobilities in column 6 are averaged, the intrinsic mobility of dsA5 is found to be $(4.6 \pm 0.2) \times 10^{-4}$ $cm^2\ V^{-1}\ s^{-1}$, regardless of the buffer in which the measurements are made. This mobility is significantly higher than the intrinsic mobilities of cAMP, 2.0×10^{-4} $cm^2\ V^{-1}\ s^{-1}$, and ACA, 2.2×10^{-4} $cm^2\ V^{-1}\ s^{-1}$ (E.S. and N.C.S., manuscript in preparation). One might have expected the mobilities of cAMP and ACA to be comparable to the mobility of dsA5, because the charge/mass ratios of the three analytes are very similar. The significantly higher intrinsic mobility observed for dsA5 suggests that the oligonucleotide is more polarizable than cAMP or ACA, probably because of counterion condensation (Manning, 1978) and the proximity of the condensed counterions to the helix axis. The greater polarizability of dsA5 would increase its effective dipole moment, increasing its interaction with the electric field (Stellwagen et al., 2001) and, consequently, the observed electrophoretic mobility.

Relatively few attempts have been made to measure the electrophoretic mobility of DNA as a function of ionic strength and determine the intrinsic mobility. Costantino et al. (1964) reported an intrinsic mobility of 7.5×10^{-4} $cm^2\ V^{-1}\ s^{-1}$ (corrected to 20°C, the temperature of the present measurements) for calf thymus DNA in NaCl, measured in a Tiselius electrophoresis cell. Electrokinetic sonic amplitude (Rasmusson and Åkerman, 1998) and electrophoretic light scattering (Hartford and Flygare, 1975) methods have also been used to measure the ionic strength dependence of the mobility of calf thymus DNA in NaCl solutions. Linear extrapolation of the reported mobilities to zero ionic strength leads to estimated intrinsic mobilities of (6.0 and 7.0) $\times 10^{-4}$ $cm^2\ V^{-1}\ s^{-1}$ for calf thymus DNA, respectively, close to the value reported by Costantino et al. (1964). These values are all much larger than the value of $(4.6 \pm 0.2) \times 10^{-4}$ $cm^2\ V^{-1}\ s^{-1}$ reported here for dsA5, possibly because the calf thymus studies used DNA concentrations that were three orders of magnitude higher than those used in the present studies, whereas the ionic strengths were similar.

Comparison of the mobilities observed in Tris and DM buffers with theoretical equations based on $I^{1/2}$

The Henry equation

Electrophoretic mobilities were calculated for dsA5 in TA and NaDM buffers using the Henry equation, Eq. 6. The charge on the DNA molecules, Q, was assumed to be the formal charge, equivalent to 38 times the elementary charge (because the 5′ residues in each strand of dsA5 are not phosphorylated). If the radius of the DNA, a, is assumed to be the radius of an equivalent sphere with volume equal to that of a right circular cylinder large enough to contain a 20-bp oligomer, the calculated mobilities are more than twice as large as the observed mobilities. If the effective radius is chosen to be one-half the contour length of the DNA oligomer, mobilities of the correct order of magnitude can be calculated, as shown in Fig. 5. However, the theoretical curve decreases more rapidly with $I^{1/2}$ than the observed mobilities. In addition, the theoretical curve cannot explain the mobility differences observed in different buffers. Hence, the Henry equation does not provide a satisfactory representation of DNA mobility as a function of ionic strength.

A second conclusion can be drawn from Fig. 5. Theoretical equations for electrophoretic mobility need to be compared with experiment over a wide range of ionic

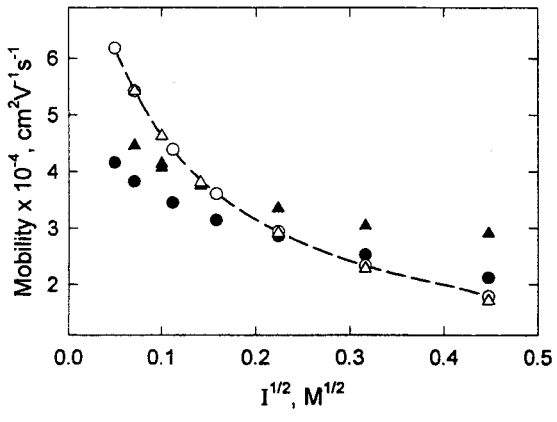

FIGURE 5 Comparison of the mobilities observed for dsA5 with the mobilities calculated from the Henry equation, Eq. 6 in: (○, ●), TA buffer, pH 8.3; and (△, ▲), NaDM buffer, pH 7.3. The solid symbols correspond to the observed mobilities; the open symbols and dashed line correspond to the calculated mobilities if the DNA radius, a, is taken to be one-half the contour length of the oligomer.

strengths before conclusions can be drawn about the agreement or disagreement of a given theory with experiment. The calculated mobilities in Fig. 5 are close to the experimental mobilities observed in 12.5 mM NaDM and 100 mM TA buffer. However, the calculated and observed mobilities do not agree at other buffer concentrations, and the shape of the theoretical curve does not agree with experiment.

The DHO equation

Fig. 6 compares the mobilities observed for dsA5 in TA and NaDM buffers with the mobilities calculated from the DHO equation, Eq. 8, using the values of $\langle \mu^o \rangle$ taken from Table 2. It can be seen that the order of magnitude of the calculated mobilities is correct, because of the use of the experimental values of $\langle \mu^o \rangle$. However, the shapes of the experimental and theoretical mobility curves are different, indicating that the mobilities observed for dsA5 in TA and NaDM buffers are poorly represented by the DHO equation.

The Pitts equation

The Pitts equation incorporates the finite size of the analyte into the DHO equation, as shown in Eqs. 9 and 10. If the term c_2 in Eq. 10 is treated as an adjustable parameter (Li et al., 1999) and set equal to 3.8, the mobilities observed for dsA5 in the four buffers studied here decrease linearly with $I^{1/2}/(1 + 3.8\ I^{1/2})$, as shown in Fig. 7. The intrinsic mobilities extrapolated to zero ionic strength are equal to those obtained from plots of the mobility or inverse mobility as a function of $I^{1/2}$ (Fig. 4), within experimental error. In addition, the slopes of the lines in Fig. 7 are approximately equal, as expected for analytes with the same effective charge (Li et al., 1999).

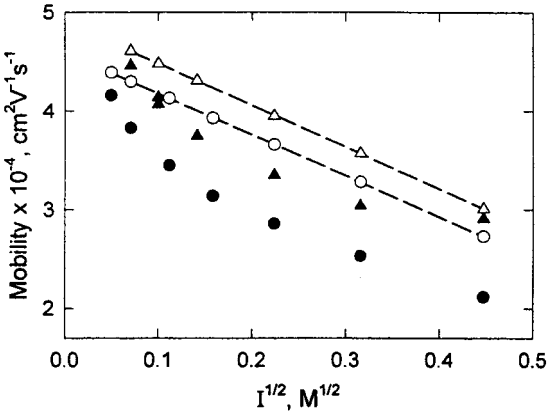

FIGURE 6 Comparison of the mobilities observed for dsA5 with the mobilities calculated from the DHO equation, Eq. 8 in: (○, ●), TA buffer, pH 8.3; and (△, ▲), NaDM buffer, pH 7.3. The solid symbols correspond to the observed mobilities; the open symbols and dashed lines correspond to the calculated mobilities.

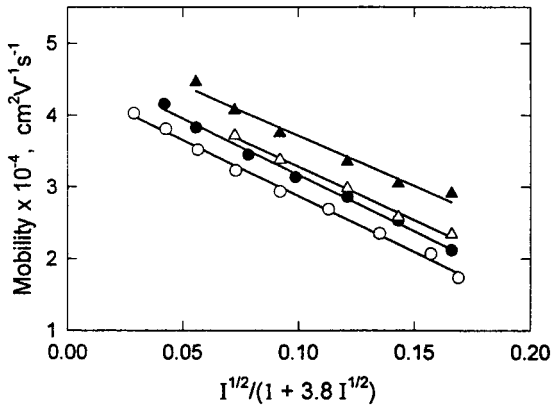

FIGURE 7 The mobilities observed for dsA5 in: (●), TA buffer, pH 8.3; (▲), NaDM buffer, pH = 7.3; (△), TrisDM buffer, pH 7.3; and (○), TAE buffer, pH 7.6, plotted as a function of $I^{1/2}/(1 + 3.8\ I^{1/2})$, according to the Pitts equation, Eq. 10.

If the term Ba in Eq. 9 is interpreted literally, the ion size parameter, a, is calculated to be 11.5 Å, inasmuch as B is a collection of constants equaling 0.329 Å^{-1} M$^{-1/2}$. This value for the ion size parameter is independent of the nature of the counterion and close to, but somewhat smaller than, the hydrated radius of the DNA helix. The ion size parameter is usually found to be somewhat smaller than the hydrated radius of the analyte, presumably because of compaction of the hydration layers around the counter- and coions by Coulombic interactions (Li et al., 1999). The linearity of the plots in Fig. 7 suggested that the Pitts equation could provide a suitable framework for describing the mobility of dsA5 as a function of ionic strength in mixed buffer/salt solutions.

The mobilities of dsA5 in 18 mM TAE buffer plus various concentrations of NaCl, and 5 mM NaDM buffer plus various concentrations of NaCl or TrisCl, were therefore calculated from Eq. 10. The values of μ^o and c_1 used in this equation were taken from Table 2; the value of c_2 was assumed to be 3.8, the value determined from the analysis of dsA5 in the same buffers without added salt (Fig. 7). A shown in Fig. 8, the mobilities calculated for dsA5 in the mixed buffer/salt solutions were very different from the experimentally observed mobilities, especially in TAE/NaCl solutions. Therefore, even though the mobilities observed for dsA5 in Tris-acetate and NaDM buffers could be linearized by plotting as a function of $I^{1/2}/(1 + c_2\ I^{1/2})$, the Pitts equation is not able to describe the mobilities observed in mixed buffer/salt solutions using the same set of adjustable parameters.

Comparison of the mobilities observed in Tris and DM buffers with the theoretical equation derived by Manning

Tris buffer with and without added NaCl

The Manning equation, Eqs. 11–13, differs from the Henry, DHO, and Pitts equations in that the mobility is predicted to

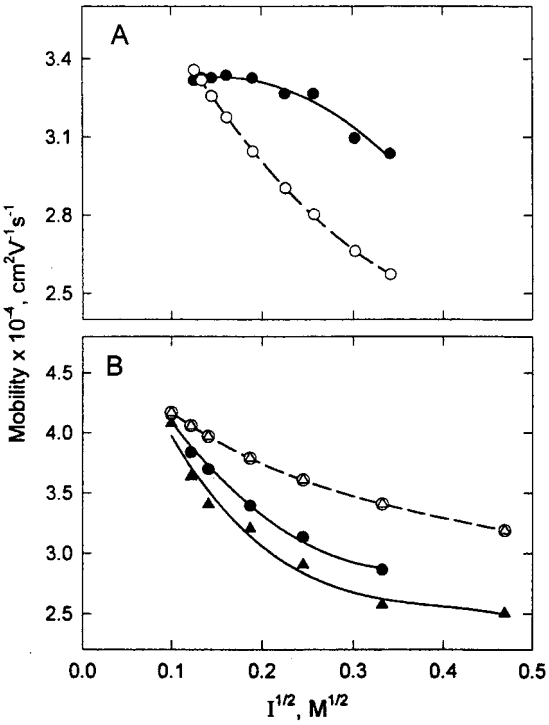

FIGURE 8 Comparison of the mobilities observed for dsA5 with the mobilities calculated from the Pitts equation, Eq. 10, in solutions containing: (*A*), (○, ●), 18 mM TAE buffer plus 1–100 mM NaCl; and (*B*), 5 mM NaDM buffer plus: (○, ●) 1–100 mM NaCl; or (△, ▲), 1–100 mM TrisCl. The solid symbols and solid lines correspond to the observed mobilities; the open symbols and dashed lines correspond to the calculated mobilities.

decrease as the logarithm of ionic strength, instead of $I^{1/2}$. Fig. 9 illustrates the dependence of the mobility of dsA5 in TAE buffers of different concentrations, and in 18 mM TAE buffer plus various concentrations of NaCl, plotted as a function of the logarithm of ionic strength. In TAE buffer, the mobility of dsA5 decreases linearly as the logarithm of ionic strength (*closed circles* and *solid line*), as predicted by the Manning equation (*open circles* and *dashed line*). The slopes of the solid and dashed lines are equal within experimental error, although the calculated mobilities are ~12% higher than the experimental values. The constant difference between the theoretical and experimental curves suggests that some parameter, not taken into account by the theory, also contributes to the observed mobilities. One such possibility is ''dielectric friction'' due to the perturbation of the moving polyion on the polarization of the surrounding medium (Schmitz, 1993); such an effect could lead to an increase in viscosity near the polyion and a corresponding reduction in the observed mobility. Alternatively, it is possible that the conductivity to be used in Eq. 13 should be that of the condensed counterions, rather than the bulk conductivity of the ions in the background electrolyte. The conductivity of the condensed counterions would be reduced because of their high concentration near the surface of the polyion (Manning, 1978), increasing the factor β in Eq. 13

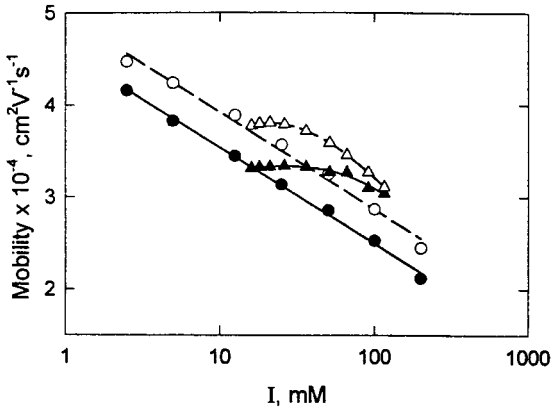

FIGURE 9 The free solution mobility of dsA5 plotted as a function of the logarithm of ionic strength, *I*, measured in solutions containing: (●), TAE buffers of various concentrations; and (▲), 18 mM TAE buffer plus 2–150 mM NaCl. The solid lines are meant to guide the eye. The dashed lines describe the mobilities calculated from the Manning equation, Eqs. 11–13, for: (○), TAE buffers of various concentrations; and (Δ), 18 mM TAE buffer plus 2–150 mM NaCl.

and decreasing the calculated mobility. Further experiments will be required to test these hypotheses.

When various concentrations of NaCl are added to 18 mM TAE buffer, the mobility of dsA5 first increases slightly, then remains constant over a wide range of ionic strengths, and finally begins to decrease when the NaCl concentration reaches ~75 mM, as shown in Fig. 9 (*solid triangles* and *continuous curved line*). This anomalous mobility plateau is observed at ionic strengths where the mobility decreases monotonically with increasing ionic strength when the solution contains Tris-acetate buffer alone (*closed circles* and *solid straight line*). It is also noteworthy that when the mobility begins to decrease at high NaCl concentrations, the rate of decrease of the mobility parallels that observed in TAE buffer alone.

The Manning electrophoresis equation captures the small increase in mobility observed upon adding small quantities of NaCl to TAE buffer, and the anomalous mobility plateau, as shown by the open triangles and dashed curve in Fig. 9. However, the calculated mobility plateau is not as broad as that observed experimentally, and the calculated mobilities at high ionic strengths decrease more rapidly with increasing ionic strength than the measured values. As a result, the calculated and measured mobilities begin to converge at high ionic strengths.

TrisDM buffer with and without added TrisCl

The mobilities observed for dsA5 in TrisDM buffer solutions of various concentrations, and 5 mM TrisDM buffer containing 5–100 mM TrisCl, are illustrated in Fig. 10 (*closed circles* and *triangles*, respectively, and *solid line*). The mobilities decrease linearly with the logarithm of the ionic strength, regardless of whether the ionic strength is

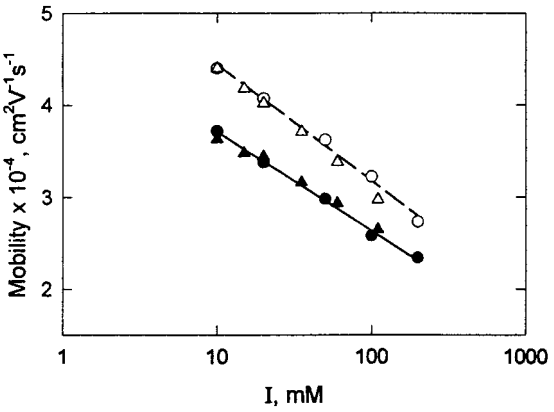

FIGURE 10 The mobility observed for dsA5 in TrisDM buffer with and without added TrisCl, compared with the mobilities calculated from the Manning equation. (●), observed mobilities in 5–100 mM TrisDM; (▲), observed mobilities in 5 mM TrisDM plus 5–100 mM TrisCl; (○), calculated mobilities in TrisDM; (△), calculated mobilities in TrisDM plus TrisCl. The lines are drawn to guide the eye.

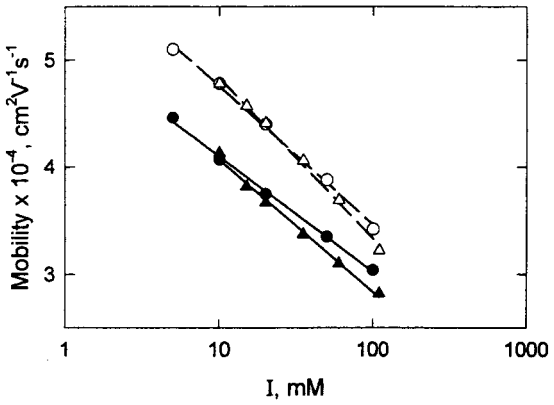

FIGURE 11 The mobility observed for dsA5 in NaDM buffer with and without added NaCl, compared with the mobilities calculated from the Manning equation. (●), observed mobilities in 2.5–100 mM NaDM; (▲), observed mobilities in 5 mM NaDM plus 5–100 mM NaCl; (○), calculated mobilities in 2.5–100 mM NaDM; (△), calculated mobilities in 5 mM NaDM plus 5–100 mM NaCl. The lines are drawn to guide the eye.

increased by increasing the TrisDM buffer concentration or the TrisCl concentration. No anomalous mobility plateau is observed in the mixed TrisDM/TrisCl solutions.

The mobilities calculated from the Manning equation for dsA5 in TrisDM and TrisDM/TrisCl solutions are shown in Fig. 10 as the open circles and triangles and the dashed line. It can be seen that the Manning equation faithfully represents the logarithmic dependence of the mobility on ionic strength in solutions containing various concentrations of TrisDM buffer and in mixed TrisDM/TrisCl solutions. On average, the calculated mobilities are ~17% higher than the corresponding experimental values. The small deviation of the calculated mobilities at high ionic strengths from the dashed line can be eliminated by correcting for the increased viscosity of solutions containing high concentrations of electrolyte (not shown).

NaDM buffer with and without added NaCl

The mobilities observed for dsA5 in NaDM buffer solutions of various concentrations, and 5 mM NaDM plus 5–100 mM NaCl, are illustrated in Fig. 11 (*filled circles* and *triangles*, respectively, with *solid lines*). It can be seen that the mobilities observed in these buffer and buffer/salt solutions also decrease linearly with the logarithm of ionic strength, although the slopes of the lines differ somewhat (compare Fig. 10). The experimental results are mirrored by the mobilities calculated from the Manning equation, as shown by the open circles and triangles and dashed lines in Fig. 11. The calculated mobilities decrease with the logarithm of ionic strength at a somewhat faster rate than observed experimentally, especially for NaDM buffer solutions containing NaCl. In addition, the calculated mobilities are ~15% higher than the experimental values.

DM buffers when the added salt has a different counterion

To try to understand the mobilities observed for dsA5 in solutions containing mixed counterions, various concentrations of NaCl were added to a constant low concentration of TrisDM buffer, and various concentrations of TrisCl were added to a constant low concentration of NaDM buffer. The results observed when TrisCl was added to NaDM are illustrated in Fig. 12 *A*. In this figure, the solid lines represent the mobility observed for dsA5 in TrisDM (*lower solid line*) and NaDM (*upper solid line*) buffer solutions of various concentrations, taken from Figs. 10 and 11. The filled circles correspond to the mobilities observed when 5–200 mM TrisCl was added to 5 mM NaDM. It can be seen that the mobility of dsA5 decreases more rapidly than expected from the mobilities observed in NaDM buffer alone. In effect, the mobility of dsA5 in NaDM "sinks" with increasing TrisCl concentration until the mobility reaches the value expected in TrisDM solutions of the same ionic strength. As a result, the mobility of an analyte cannot be predicted from the total ionic strength of the solution when the counterion in the added salt differs from that in the background buffer.

The upper and lower dashed lines in Fig. 12 *A* represent the mobilities calculated for dsA5 in NaDM and TrisDM buffers, respectively, using the Manning electrophoresis theory, as shown in Figs. 10 and 11. The open circles represent the calculated mobilities for solutions containing 5 mM NaDM and increasing concentrations of TrisCl. It can be seen that the calculated mobilities in the mixed NaDM/TrisCl solutions mirror the results observed experimentally, except that the calculated mobilities decrease somewhat more rapidly than the experimental mobilities with increasing ionic strength.

Fig. 12 *B* represents the opposite situation, the addition of increasing concentrations of NaCl to a constant low

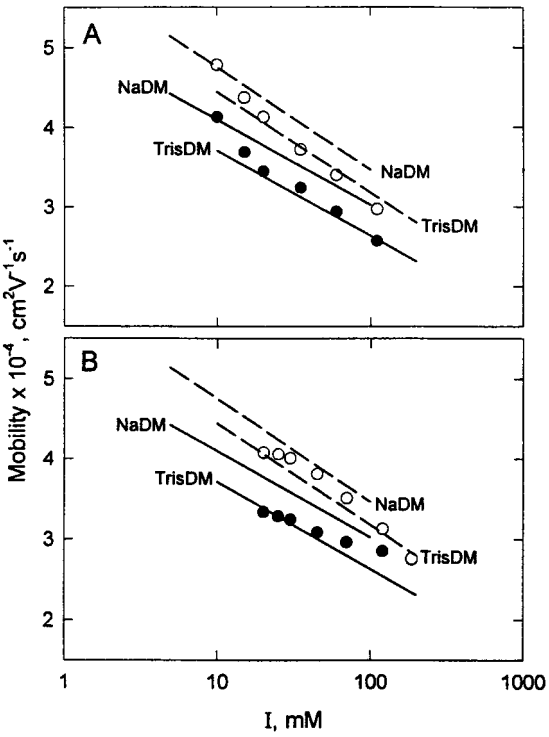

FIGURE 12 The mobility observed for dsA5 in DM buffers, compared with the mobility observed when the counterion in the added salt is different from that in the background electrolyte. (*A*) 5–100 mM TrisCl added to 5 mM NaDM. (●), experimental mobilities; (○), mobilities calculated from the Manning theory, Eqs. 11–13. (*B*) 5–167 mM NaCl added to 10 mM TrisDM; (●), experimental mobilities; (○), mobilities calculated from the Manning equation. In both *A* and *B*, the upper and lower solid lines correspond to the mobilities observed experimentally for dsA5 in NaDM and TrisDM buffers, respectively, taken from Figs. 10 and 11; the upper and lower dashed lines correspond to the mobilities calculated from the Manning equation for dsA5 in NaDM and TrisDM buffers, respectively, taken from Figs. 10 and 11.

concentration of TrisDM buffer. The filled circles correspond to the mobility observed for dsA5 when 2–167 mM NaCl was added to 10 mM TrisDM buffer. The upper and lower solid lines represent the mobilities observed for dsA5 in solutions containing various concentrations of NaDM and TrisDM buffer, respectively, taken from Figs. 10 and 11; the solid lines are the same as those in Fig. 12 *A*. It can be seen that the mobility of dsA5 decreases less rapidly with increasing ionic strength than would be expected from the results observed in TrisDM buffer alone, as the mobility of dsA5 ''walks over'' to join the curve for NaDM at high NaCl concentrations. The high conductivity of these solutions prevented experiments at still higher ionic strengths, which would have shown whether the mobilities decreased at the rate expected for solutions containing only NaDM.

The open circles in Fig. 12 *B* correspond to the mobility of dsA5 in solutions containing 10 mM TrisDM and 2–167 mM NaCl, calculated from the Manning theory, Eqs. 11–13. The upper and lower dashed lines represent the calculated mobility of dsA5 in NaDM and TrisDM buffers, respectively, taken from Figs. 10 and 11. It can be seen that the calculated mobilities are nearly constant when the NaCl concentration is 20 mM or less, and then decrease at higher NaCl concentrations. The mobilities calculated for dsA5 in the mixed NaCl/TrisDM solutions are between the mobilities calculated in NaDM and TrisDM buffers alone, as observed experimentally (*filled circles* in Fig. 12 *B*). However, the shapes of the calculated and experimental mobility curves do not agree because of the ''downturn'' in the calculated mobilities at ionic strengths greater than ~50 mM. A similar ''downturn'' in the calculated mobilities is observed in Fig. 9, when high concentrations of NaCl are added to TAE buffer.

The results suggest that some factor, not taken into account in the theory, is affecting the mobilities observed when Na^+ ions are added to Tris buffer solutions. In TAE and TrisDM buffers, but not in NaDM buffers, both the anion and cation are buffering ions. This difference may affect the buffer composition within the sample zone, especially if the pH of the sample is somewhat different from that of the background electrolyte (Andersson and Hägglund, 2002). The addition of Na^+ ions to Tris buffers would increase the ionic strength of the solution, decreasing the calculated mobility without affecting the exchange of buffering ions across both edges of the sample zone, which may contribute to the observed mobilities.

It has previously been shown that the electrophoretic mobility of DNA in TAE buffers and in NaCl solutions of the same ionic strength are very similar, suggesting that Na^+ and $Tris^+$ ions are condensed about the DNA helix to a similar extent (Stellwagen et al., 1997). Similar conclusions have been reached from NMR measurements (Anderson et al., 1978). Despite this apparent similarity, numerical calculations of the mobility of short DNA oligomers using boundary element methods found that the calculated mobility only agreed with experiment if it was assumed that 40% of the net charge on the DNA phosphates was neutralized by the site binding of $Tris^+$ ions to the phosphate residues, or the net charge on the DNA was substantially reduced (Mazur et al., 2001). Comparative studies with a variety of counterions are needed to assess the role of the counterion in the electrostatic shielding of DNA. Such studies are under way in this laboratory.

CONCLUDING REMARKS

The results described here have shown that the free solution electrophoretic mobility of DNA decreases linearly with the logarithm of ionic strength, over a nearly 200-fold range of ionic strengths, when the ionic strength of the solution is increased by increasing the buffer concentration or by adding a uni-univalent salt having the same counterion as the counterion in the buffer. The present study has been carried out with a small 20-bp oligomer, dsA5, but very similar results have been observed for a much larger DNA, linear pUC19 (2868 bp) in TAE buffer (Stellwagen and Stell-

wagen, 2002). Hence, the electrostatic shielding effects described here are expected to apply to DNA molecules of various molecular weights, as well as to other highly charged polyions.

The decrease in mobility of dsA5 with increasing ionic strength was very similar in TAE, NaDM, and TrisDM buffers of various concentrations, solutions containing NaDM plus various concentrations of NaCl and solutions containing TrisDM plus various concentrations of TrisCl. Hence, the decrease in the free solution mobility with increasing ionic strength must be attributed to general electrostatic screening of the DNA by the ions in the diffuse ion atmosphere. The actual mobility observed for dsA5 at a given ionic strength depends somewhat on the specific buffer or buffer/salt solution in which the measurements are made, because of the different conductivities (or transference numbers) of the various buffer and salt ions. These effects are not easy to predict because of the concentration dependence of the transference numbers of the buffer ions (Štědrý et al., 1996). For this reason, the observed mobility is a function of the total number of ions in the solution, as well as their limiting ionic conductivities. In addition, the degree of dissociation of weak buffer ions, and hence the pH at the boundaries of the sample zone, may be concentration dependent.

Anomalous electrophoretic mobilities are observed for dsA5 when the ionic strength of the solution is increased by adding a uni-univalent salt with a counterion different from that in the buffer. In such solutions, the mobility of DNA decreases either more rapidly or more slowly with increasing ionic strength than expected, depending on whether the limiting equivalent conductivity of the cation in the added salt is lower or higher than the limiting equivalent conductivity of the buffer cation. The results demonstrate that the intrinsic mobility observed for DNA at finite ionic strengths is modulated by the relative concentrations and mobilities of all the ions in the solution.

The ionic strength dependence of the mobilities observed for dsA5 in various buffer and buffer/salt solutions is well described by the simple Manning theory of electrophoresis, even in buffer/salt mixtures with different cations. This is a remarkable result, considering that the equation contains no adjustable parameters and the theory was derived for high molecular weight DNA molecules, not the small oligomer studied here. The results suggest that the Manning theory of electrophoresis incorporates most of the factors responsible for the electrostatic shielding of DNA in solutions containing small electrolytes. However, it must also be noted that quantitative agreement between theory and experiment has not been achieved, because the calculated mobilities are ~8–20% higher than the observed mobilities. It seems likely that some other factor, such as the concentration dependence of the transference numbers of the ionic components in the solution, or the effect of electrolyte friction (Schmitz, 1993) will need to be incorporated into the theory to achieve better agreement.

Attempts were also made to fit the mobility data to the Henry, DHO, and Pitts equations for electrophoresis, all of which predict that the mobility should decrease as the square root of ionic strength. The Henry and DHO equations were not able to fit the mobility data when the ionic strength of the solution was varied by changing the buffer concentration. The Pitts equation was able to linearize the mobilities observed for dsA5 in the four buffers used here, using an additional adjustable parameter. However, when the same parameter was used to calculate the mobility of dsA5 in mixed buffer/salt solutions, the calculated mobilities did not agree with experiment. Hence, the conclusion must be drawn that the electrophoretic mobility of DNA and other highly charged polyelectrolytes cannot be described by the Debye-Hückel equation or its variants. The reason is clear—the electrophoretic mobility of DNA decreases as the logarithm of ionic strength, as predicted by the Manning theory, not the square root of ionic strength, as predicted by Debye-Hückel-type theories.

The final point to be made from the studies presented here is that it is not sufficient to compare theory and experiment at one or a few ionic strengths. To determine whether various theories of electrophoresis provide a good description of the phenomenon, and to understand the factors contributing to the electrostatic shielding of DNA, theory and experiment must be compared over a wide range of ionic strengths.

The expert technical assistance of Qian Dong is acknowledged.

Financial support of this work from the National Institute of General Medical Sciences, grants GM29690 and GM61009 (to N.C.S.), is gratefully acknowledged.

REFERENCES

Allison, S. A., and S. Mazur. 1998. Modeling the free solution electrophoretic mobility of short DNA fragments. *Biopolymers*. 46:359–373.

Anderson, C. F., M. T. Record Jr., and P. A. Hart. 1978. Sodium-23 NMR studies of cation-DNA interactions. *Biophys. Chem.* 7:301–316.

Andersson, E. K., and I. Hägglund. 2002. Increase of sample load without peak deterioration by careful selection of electrolyte in capillary zone electrophoresis. *J. Chromatogr. A*. 953:227–237.

Beckers, J. L., and P. Boček. 2000. Sample stacking in capillary zone electrophoresis: principles, advantages and limitations. *Electrophoresis*. 21:2747–2767.

Beckers, J. L., P. Gebauer, and P. Boček. 2001. System zones in capillary zone electrophoresis. *Electrophoresis*. 22:3648–3658.

Bockris, J. O'M., and A. K. N. Reddy. 1998. Modern Electrochemistry Ionics, 2nd ed, Vol. 1. Plenum Press, New York.

Costantino, L., A. M. Liquori, and V. Vitagliano. 1964. Influence of thermal denaturation on the electrophoretic mobility of calf thymus DNA. *Biopolymers*. 2:1–8.

Friedl, S., J. C. Reijenga, and E. Kenndler. 1995. Ionic strength and charge number correction for mobilities of multivalent organic anions in capillary electrophoresis. *J. Chromatogr. A*. 709:163–170.

Gebauer, P., and P. Boček. 1997. System peaks in capillary zone electrophoresis. I. Simple model of vacancy electrophoresis. *J. Chromatogr. A*. 772:73–79.

Good, N. E., G. D. Winget, W. Winter, T. N. Connolly, S. Izawa, and R. M. M. Singh. 1966. Hydrogen ion buffers for biological research. *Biochemistry*. 5:467–477.

Grossman, P. D. 1992. Factors affecting the performance of capillary electrophoresis separations: Joule heating, electroosmosis, and zone dispersion. *In* Capillary Electrophoresis, Theory and Practice. P. D. Grossman and J. C. Colburn, editors. Academic Press, San Diego. 3–43.

Hartford, S. L., and W. H. Flygare. 1975. Electrophoretic light scattering on calf thymus deoxyribonucleic acid and tobacco mosaic virus. *Macromolecules*. 8:80–83.

Henry, D. C. 1931. The cataphoresis of suspended particles. Part I. The equation of cataphoresis. *Proc. Roy. Soc. A*. 133:106–129.

Jumppanen, J. H., and M. L. Riekkola. 1995. Influence of electrolyte composition on the effective electric field strength in capillary zone electrophoresis. *Electrophoresis*. 16:1441–1444.

Klein, S. D., and R. G. Bates. 1980. Conductance of tris(hydroxymethyl) aminomethane hydrochloride (Tris·HCl) in water at 25 and 37°C. *J. Soln. Chem*. 9:289–292.

Li, D., S. Fu, and C. A. Lucy. 1999. Prediction of electrophoretic mobilities. 3. Effect of ionic strength in capillary zone electrophoresis. *Anal. Chem*. 71:687–699.

Manning, G. 1978. The molecular theory of polyelectrolyte solutions with applications to the electrostatic properties of polynucleotides. *Q. Rev. Biophys*. 11:179–246.

Manning, G. 1981. Limiting laws and counterion condensation in polyelectrolyte solutions. 7. Electrophoretic mobility and conductance. *J. Phys. Chem*. 85:1506–1515.

Mazur, S., C. Chen, and S. A. Allison. 2001. Modeling the electrophoresis of short duplex DNA: counterions K^+ and $Tris^+$. *J. Phys. Chem. B*. 105:1100–1108.

Ng, B., and P. H. Barry. 1995. The measurement of ionic conductivities and mobilities of certain less common organic ions needed for junction potential corrections in electrophysiology. *J. Neuroscience Meth*. 56:37–41.

Nkodo, A. E., J. M. Garnier, B. Tinland, H. Ren, C. Desruisseaux, L. C. McCormick, G. Drouin, and G. W. Slater. 2001. Diffusion coefficient of DNA molecules during free solution electrophoresis. *Electrophoresis*. 22:2424–2432.

Onsager, L., and R. M. Fuoss. 1932. Irreversible processes in electrolytes. Diffusion, conductance, and viscous flow in arbitrary mixtures of strong electrolytes. *J. Phys. Chem*. 36:2689–2778.

Overbeek, J. T. G., and P. H. Wiersema. 1967. The interpretation of electrophoretic mobilities. *In* Electrophoresis. M. Bier, editor. Academic Press, New York. 1–52.

Pitts, E. 1953. An extension of the theory of the conductivity and viscosity of electrolyte solutions. *Proc. Roy. Soc. A*. 217:43–70.

Pitts, E., B. E. Tabor, and J. Daly. 1970. Concentration dependence of electrolyte conductance. 2. Comparison of experimental data with the Fuoss-Onsager and Pitts treatments. *Trans. Faraday Soc*. 66:693–707.

Porras, S. P., M. L. Riekkola, and E. Kenndler. 2002. Capillary electrophoresis of anionic analytes in methanol: effect of counter-ions on electrophoretic mobility. *Electrophoresis*. 23:367–374.

Rasmusson, M. and B. Åkerman. 1998. Dynamic mobility of DNA. *Langmuir*. 14:3512–3516.

Reijenga, J. D., and E. J. Kenndler. 1994. Computational simulation of migration and dispersion in free capillary zone electrophoresis I. Description of the theoretical model. *J. Chromatogr. A*. 659:403–415.

Russel, W. B., D. A. Saville, and W. R. Schowalter. 1989. Colloidal Dispersions. Cambridge University Press, Cambridge.

Schellman, J. A., and D. Stigter. 1977. Electrical double layer, zeta potential, and electrophoretic charge of double-stranded DNA. *Biopolymers*. 16:1415–1434.

Schmitz, K. S. 1993. Macroions in Solution and Colloidal Suspension. VCH Publishers, New York.

Sober, H. A., editor. 1968. CRC Handbook of Biochemistry. The Chemical Rubber Co., Cleveland. J-156.

Southern, E. M. 1979. Measurement of DNA length by gel electrophoresis. *Anal. Biochem*. 100:319–323.

Štědrý, M., Š. Popelka, B. Gaš, and E. Kenndler. 1996. Influence of transference number on migration and deformation of concentration boundaries in capillary zone electrophoresis. *Electrophoresis*. 17:1121–1125.

Stellwagen, N. C. 1998. DNA gel electrophoresis. *In* Nucleic Acid Electrophoresis. D. Tietz, editor. Springer, New York. 1–53.

Stellwagen, N. C., A. Bossi, C. Gelfi, and P. G. Righetti. 2001. Do orientation effects contribute to the molecular weight dependence of the free solution mobility of DNA? *Electrophoresis*. 22:4311–4315.

Stellwagen, N. C., C. Gelfi, and P. G. Righetti. 1997. The free solution mobility of DNA. *Biopolymers*. 42:687–703.

Stellwagen, E., and N. C. Stellwagen. 2002. The free solution mobility of DNA in Tris-acetate-EDTA buffers of different concentrations, with and without added NaCl. *Electrophoresis*. 23:1935–1941.

Van Winkle, D., A. Beheshti, and R. L. Rill. 2002. DNA electrophoresis in agarose gels: a simple relation describing the length dependence of mobility. *Electrophoresis*. 23:15–19.

Viovy, J. L. 2000. Electrophoresis of DNA and other polyelectrolytes: physical mechanisms. *Rev. Modern Phys*. 72:813–872.

Weast, R. C., editor. 1984. CRC Handbook of Chemistry and Physics, 65th ed. CRC Press, Boca Raton, FL. D-255–D-268, D-171–D-173.

Weime, R. J. 1975. Theory of electrophoresis. *In* Chromatography, 3rd ed. E. Heftmann, editor. Van Nostrand Reinhold, New York. 228–281.